



University of
Massachusetts
Amherst

**Branching fraction measurements of
charged B decays to K^*+K+K^- , $K^*+\pi K^-$
 $+(-)$, $K^*+K+\pi(-)$ and $K^*+\pi(+)\pi(-)$ final states**

Item Type	article
DOI	10.1103/PhysRevD.74.051104
Download date	2026-05-13 03:47:07
Link to Item	https://hdl.handle.net/20.500.14394/5427

Branching fraction measurements of charged B decays to $K^{*+} K^+ K^-$, $K^{*+} \pi^+ K^-$, $K^{*+} K^+ \pi^-$ and $K^{*+} \pi^+ \pi^-$ final states

B. Aubert,¹ R. Barate,¹ M. Bona,¹ D. Boutigny,¹ F. Couderc,¹ Y. Karyotakis,¹ J. P. Lees,¹ V. Poireau,¹ V. Tisserand,¹ A. Zghiche,¹ E. Grauges,² A. Palano,³ J. C. Chen,⁴ N. D. Qi,⁴ G. Rong,⁴ P. Wang,⁴ Y. S. Zhu,⁴ G. Eigen,⁵ I. Ofte,⁵ B. Stugu,⁵ G. S. Abrams,⁶ M. Battaglia,⁶ D. N. Brown,⁶ J. Button-Shafer,⁶ R. N. Cahn,⁶ E. Charles,⁶ M. S. Gill,⁶ Y. Groyzman,⁶ R. G. Jacobsen,⁶ J. A. Kadyk,⁶ L. T. Kerth,⁶ Yu. G. Kolomensky,⁶ G. Kukartsev,⁶ G. Lynch,⁶ L. M. Mir,⁶ T. J. Orimoto,⁶ M. Pripstein,⁶ N. A. Roe,⁶ M. T. Ronan,⁶ W. A. Wenzel,⁶ P. del Amo Sanchez,⁷ M. Barrett,⁷ K. E. Ford,⁷ T. J. Harrison,⁷ A. J. Hart,⁷ C. M. Hawkes,⁷ S. E. Morgan,⁷ A. T. Watson,⁷ T. Held,⁸ H. Koch,⁸ B. Lewandowski,⁸ M. Pelizaeus,⁸ K. Peters,⁸ T. Schroeder,⁸ M. Steinke,⁸ J. T. Boyd,⁹ J. P. Burke,⁹ W. N. Cottingham,⁹ D. Walker,⁹ T. Cuhadar-Donszelmann,¹⁰ B. G. Fulsom,¹⁰ C. Hearty,¹⁰ N. S. Knecht,¹⁰ T. S. Mattison,¹⁰ J. A. McKenna,¹⁰ A. Khan,¹¹ P. Kyberd,¹¹ M. Saleem,¹¹ D. J. Sherwood,¹¹ L. Teodorescu,¹¹ V. E. Blinov,¹² A. D. Bukin,¹² V. P. Druzhinin,¹² V. B. Golubev,¹² A. P. Onuchin,¹² S. I. Serednyakov,¹² Yu. I. Skovpen,¹² E. P. Solodov,¹² K. Yu Todyshev,¹² D. S. Best,¹³ M. Bondioli,¹³ M. Bruinsma,¹³ M. Chao,¹³ S. Curry,¹³ I. Eschrich,¹³ D. Kirkby,¹³ A. J. Lankford,¹³ P. Lund,¹³ M. Mandelkern,¹³ R. K. Mommsen,¹³ W. Roethel,¹³ D. P. Stoker,¹³ S. Abachi,¹⁴ C. Buchanan,¹⁴ S. D. Foulkes,¹⁵ J. W. Gary,¹⁵ O. Long,¹⁵ B. C. Shen,¹⁵ K. Wang,¹⁵ L. Zhang,¹⁵ H. K. Hadavand,¹⁶ E. J. Hill,¹⁶ H. P. Paar,¹⁶ S. Rahatlou,¹⁶ V. Sharma,¹⁶ J. W. Berryhill,¹⁷ C. Campagnari,¹⁷ A. Cunha,¹⁷ B. Dahmes,¹⁷ T. M. Hong,¹⁷ D. Kovalskyi,¹⁷ J. D. Richman,¹⁷ T. W. Beck,¹⁸ A. M. Eisner,¹⁸ C. J. Flacco,¹⁸ C. A. Heusch,¹⁸ J. Kroseberg,¹⁸ W. S. Lockman,¹⁸ G. Nesom,¹⁸ T. Schalk,¹⁸ B. A. Schumm,¹⁸ A. Seiden,¹⁸ P. Spradlin,¹⁸ D. C. Williams,¹⁸ M. G. Wilson,¹⁸ J. Albert,¹⁹ E. Chen,¹⁹ A. Dvoretzskii,¹⁹ F. Fang,¹⁹ D. G. Hitlin,¹⁹ I. Narsky,¹⁹ T. Piatenko,¹⁹ F. C. Porter,¹⁹ A. Ryd,¹⁹ A. Samuel,¹⁹ G. Mancinelli,²⁰ B. T. Meadows,²⁰ K. Mishra,²⁰ M. D. Sokoloff,²⁰ F. Blanc,²¹ P. C. Bloom,²¹ S. Chen,²¹ W. T. Ford,²¹ J. F. Hirschauer,²¹ A. Kreisel,²¹ M. Nagel,²¹ U. Nauenberg,²¹ A. Olivas,²¹ W. O. Ruddick,²¹ J. G. Smith,²¹ K. A. Ulmer,²¹ S. R. Wagner,²¹ J. Zhang,²¹ A. Chen,²² E. A. Eckhart,²² A. Soffer,²² W. H. Toki,²² R. J. Wilson,²² F. Winklmeier,²² Q. Zeng,²² D. D. Altenburg,²³ E. Feltresi,²³ A. Hauke,²³ H. Jasper,²³ A. Petzold,²³ B. Spaan,²³ T. Brandt,²⁴ V. Klose,²⁴ H. M. Lacker,²⁴ W. F. Mader,²⁴ R. Nogowski,²⁴ J. Schubert,²⁴ K. R. Schubert,²⁴ R. Schwierz,²⁴ J. E. Sundermann,²⁴ A. Volk,²⁴ D. Bernard,²⁵ G. R. Bonneaud,²⁵ P. Grenier,^{25,*} E. Latour,²⁵ Ch. Thiebaux,²⁵ M. Verderi,²⁵ P. J. Clark,²⁶ W. Gradl,²⁶ F. Muheim,²⁶ S. Playfer,²⁶ A. I. Robertson,²⁶ Y. Xie,²⁶ M. Andreotti,²⁷ D. Bettoni,²⁷ C. Bozzi,²⁷ R. Calabrese,²⁷ G. Cibinetto,²⁷ E. Luppi,²⁷ M. Negrini,²⁷ A. Petrella,²⁷ L. Piemontese,²⁷ E. Prencipe,²⁷ F. Anulli,²⁸ R. Baldini-Feroli,²⁸ A. Calcaterra,²⁸ R. de Sangro,²⁸ G. Finocchiaro,²⁸ S. Pacetti,²⁸ P. Patteri,²⁸ I. M. Peruzzi,^{28,†} M. Piccolo,²⁸ M. Rama,²⁸ A. Zallo,²⁸ A. Buzzo,²⁹ R. Capra,²⁹ R. Contri,²⁹ M. Lo Vetere,²⁹ M. M. Macri,²⁹ M. R. Monge,²⁹ S. Passaggio,²⁹ C. Patrignani,²⁹ E. Robutti,²⁹ A. Santroni,²⁹ S. Tosi,²⁹ G. Brandenburg,³⁰ K. S. Chaisanguanthum,³⁰ M. Morii,³⁰ J. Wu,³⁰ R. S. Dubitzky,³¹ J. Marks,³¹ S. Schenk,³¹ U. Uwer,³¹ W. Bhimji,³² D. A. Bowerman,³² P. D. Dauncey,³² U. Egede,³² R. L. Flack,³² J. A. Nash,³² M. B. Nikolich,³² W. Panduro Vazquez,³² P. K. Behera,³³ X. Chai,³³ M. J. Charles,³³ U. Mallik,³³ N. T. Meyer,³³ V. Ziegler,³³ J. Cochran,³⁴ H. B. Crawley,³⁴ L. Dong,³⁴ V. Eyges,³⁴ W. T. Meyer,³⁴ S. Prell,³⁴ E. I. Rosenberg,³⁴ A. E. Rubin,³⁴ A. V. Gritsan,³⁵ A. G. Denig,³⁶ M. Fritsch,³⁶ G. Schott,³⁶ N. Arnaud,³⁷ M. Davier,³⁷ G. Grosdidier,³⁷ A. Höcker,³⁷ F. Le Diberder,³⁷ V. Lepeltier,³⁷ A. M. Lutz,³⁷ A. Oyanguren,³⁷ S. Pruvot,³⁷ S. Rodier,³⁷ P. Roudeau,³⁷ M. H. Schune,³⁷ A. Stocchi,³⁷ W. F. Wang,³⁷ G. Wormser,³⁷ C. H. Cheng,³⁸ D. J. Lange,³⁸ D. M. Wright,³⁸ C. A. Chavez,³⁹ I. J. Forster,³⁹ J. R. Fry,³⁹ E. Gabathuler,³⁹ R. Gamet,³⁹ K. A. George,³⁹ D. E. Hutchcroft,³⁹ D. J. Payne,³⁹ K. C. Schofield,³⁹ C. Touramanis,³⁹ A. J. Bevan,⁴⁰ F. Di Lodovico,⁴⁰ W. Menges,⁴⁰ R. Sacco,⁴⁰ G. Cowan,⁴¹ H. U. Flaecher,⁴¹ D. A. Hopkins,⁴¹ P. S. Jackson,⁴¹ T. R. McMahon,⁴¹ S. Ricciardi,⁴¹ F. Salvatore,⁴¹ A. C. Wren,⁴¹ D. N. Brown,⁴² C. L. Davis,⁴² J. Allison,⁴³ N. R. Barlow,⁴³ R. J. Barlow,⁴³ Y. M. Chia,⁴³ C. L. Edgar,⁴³ G. D. Lafferty,⁴³ M. T. Naisbit,⁴³ J. C. Williams,⁴³ J. I. Yi,⁴³ C. Chen,⁴⁴ W. D. Hulsbergen,⁴⁴ A. Jawahery,⁴⁴ C. K. Lae,⁴⁴ D. A. Roberts,⁴⁴ G. Simi,⁴⁴ G. Blaylock,⁴⁵ C. Dallapiccola,⁴⁵ S. S. Hertzbach,⁴⁵ X. Li,⁴⁵ T. B. Moore,⁴⁵ S. Saremi,⁴⁵ H. Staengle,⁴⁵ R. Cowan,⁴⁶ G. Sciolla,⁴⁶ S. J. Sekula,⁴⁶ M. Spitznagel,⁴⁶ F. Taylor,⁴⁶ R. K. Yamamoto,⁴⁶ H. Kim,⁴⁷ S. E. Mclachlin,⁴⁷ P. M. Patel,⁴⁷ S. H. Robertson,⁴⁷ A. Lazzaro,⁴⁸ V. Lombardo,⁴⁸ F. Palombo,⁴⁸ J. M. Bauer,⁴⁹ L. Cremaldi,⁴⁹ V. Eschenburg,⁴⁹ R. Godang,⁴⁹ R. Kroeger,⁴⁹ D. A. Sanders,⁴⁹ D. J. Summers,⁴⁹ H. W. Zhao,⁴⁹ S. Brunet,⁵⁰ D. Côté,⁵⁰ M. Simard,⁵⁰ P. Taras,⁵⁰ F. B. Viaud,⁵⁰ H. Nicholson,⁵¹ N. Cavallo,^{52,‡} G. De Nardo,⁵² F. Fabozzi,^{52,‡} C. Gatto,⁵² L. Lista,⁵² D. Monorchio,⁵² P. Paolucci,⁵² D. Piccolo,⁵² C. Sciacca,⁵² M. Baak,⁵³ G. Raven,⁵³ H. L. Snoek,⁵³ C. P. Jessop,⁵⁴ J. M. LoSecco,⁵⁴ T. Allmendinger,⁵⁵ G. Benelli,⁵⁵ K. K. Gan,⁵⁵ K. Honscheid,⁵⁵ D. Hufnagel,⁵⁵ P. D. Jackson,⁵⁵ H. Kagan,⁵⁵ R. Kass,⁵⁵ A. M. Rahimi,⁵⁵ R. Ter-Antonyan,⁵⁵ Q. K. Wong,⁵⁵ N. L. Blount,⁵⁶ J. Brau,⁵⁶ R. Frey,⁵⁶ O. Igonkina,⁵⁶ M. Lu,⁵⁶ R. Rahmat,⁵⁶ N. B. Sinev,⁵⁶ D. Strom,⁵⁶ J. Strube,⁵⁶ E. Torrence,⁵⁶ A. Gaz,⁵⁷ M. Margoni,⁵⁷

M. Morandin,⁵⁷ A. Pompili,⁵⁷ M. Posocco,⁵⁷ M. Rotondo,⁵⁷ F. Simonetto,⁵⁷ R. Stroili,⁵⁷ C. Voci,⁵⁷ M. Benayoun,⁵⁸ J. Chauveau,⁵⁸ H. Briand,⁵⁸ P. David,⁵⁸ L. Del Buono,⁵⁸ Ch. de la Vaissière,⁵⁸ O. Hamon,⁵⁸ B. L. Hartfiel,⁵⁸ M. J. J. John,⁵⁸ Ph. Leruste,⁵⁸ J. Malclès,⁵⁸ J. Ocariz,⁵⁸ L. Roos,⁵⁸ G. Therin,⁵⁸ L. Gladney,⁵⁹ J. Panetta,⁵⁹ M. Biasini,⁶⁰ R. Covarelli,⁶⁰ C. Angelini,⁶¹ G. Batignani,⁶¹ S. Bettarini,⁶¹ F. Bucci,⁶¹ G. Calderini,⁶¹ M. Carpinelli,⁶¹ R. Cenci,⁶¹ F. Forti,⁶¹ M. A. Giorgi,⁶¹ A. Lusiani,⁶¹ G. Marchiori,⁶¹ M. A. Mazur,⁶¹ M. Morganti,⁶¹ N. Neri,⁶¹ G. Rizzo,⁶¹ J. J. Walsh,⁶¹ M. Haire,⁶² D. Judd,⁶² D. E. Wagoner,⁶² J. Biesiada,⁶³ N. Danielson,⁶³ P. Elmer,⁶³ Y. P. Lau,⁶³ C. Lu,⁶³ J. Olsen,⁶³ A. J. S. Smith,⁶³ A. V. Telnov,⁶³ F. Bellini,⁶⁴ G. Cavoto,⁶⁴ A. D’Orazio,⁶⁴ D. del Re,⁶⁴ E. Di Marco,⁶⁴ R. Faccini,⁶⁴ F. Ferrarotto,⁶⁴ F. Ferroni,⁶⁴ M. Gaspero,⁶⁴ L. Li Gioi,⁶⁴ M. A. Mazzoni,⁶⁴ S. Morganti,⁶⁴ G. Piredda,⁶⁴ F. Polci,⁶⁴ F. Safai Tehrani,⁶⁴ C. Voena,⁶⁴ M. Ebert,⁶⁵ H. Schröder,⁶⁵ R. Waldi,⁶⁵ T. Adye,⁶⁶ N. De Groot,⁶⁶ B. Franek,⁶⁶ E. O. Olaiya,⁶⁶ F. F. Wilson,⁶⁶ R. Aleksan,⁶⁷ S. Emery,⁶⁷ A. Gaidot,⁶⁷ S. F. Ganzhur,⁶⁷ G. Hamel de Monchenault,⁶⁷ W. Kozanecki,⁶⁷ M. Legendre,⁶⁷ G. Vasseur,⁶⁷ Ch. Yèche,⁶⁷ M. Zito,⁶⁷ X. R. Chen,⁶⁸ H. Liu,⁶⁸ W. Park,⁶⁸ M. V. Purohit,⁶⁸ J. R. Wilson,⁶⁸ M. T. Allen,⁶⁹ D. Aston,⁶⁹ R. Bartoldus,⁶⁹ P. Bechtel,⁶⁹ N. Berger,⁶⁹ R. Claus,⁶⁹ J. P. Coleman,⁶⁹ M. R. Convery,⁶⁹ M. Cristinziani,⁶⁹ J. C. Dingfelder,⁶⁹ J. Dorfan,⁶⁹ G. P. Dubois-Felsmann,⁶⁹ D. Dujmic,⁶⁹ W. Dunwoodie,⁶⁹ R. C. Field,⁶⁹ T. Glanzman,⁶⁹ S. J. Gowdy,⁶⁹ M. T. Graham,⁶⁹ V. Halyo,⁶⁹ C. Hast,⁶⁹ T. Hryn’ova,⁶⁹ W. R. Innes,⁶⁹ M. H. Kelsey,⁶⁹ P. Kim,⁶⁹ D. W. G. S. Leith,⁶⁹ S. Li,⁶⁹ S. Luitz,⁶⁹ V. Luth,⁶⁹ H. L. Lynch,⁶⁹ D. B. MacFarlane,⁶⁹ H. Marsiske,⁶⁹ R. Messner,⁶⁹ D. R. Muller,⁶⁹ C. P. O’Grady,⁶⁹ V. E. Ozcan,⁶⁹ A. Perazzo,⁶⁹ M. Perl,⁶⁹ T. Pulliam,⁶⁹ B. N. Ratcliff,⁶⁹ A. Roodman,⁶⁹ A. A. Salnikov,⁶⁹ R. H. Schindler,⁶⁹ J. Schwiening,⁶⁹ A. Snyder,⁶⁹ J. Stelzer,⁶⁹ D. Su,⁶⁹ M. K. Sullivan,⁶⁹ K. Suzuki,⁶⁹ S. K. Swain,⁶⁹ J. M. Thompson,⁶⁹ J. Va’vra,⁶⁹ N. van Bakel,⁶⁹ M. Weaver,⁶⁹ A. J. R. Weinstein,⁶⁹ W. J. Wisniewski,⁶⁹ M. Wittgen,⁶⁹ D. H. Wright,⁶⁹ A. K. Yarritu,⁶⁹ K. Yi,⁶⁹ C. C. Young,⁶⁹ P. R. Burchat,⁷⁰ A. J. Edwards,⁷⁰ S. A. Majewski,⁷⁰ B. A. Petersen,⁷⁰ C. Roat,⁷⁰ L. Wilden,⁷⁰ S. Ahmed,⁷¹ M. S. Alam,⁷¹ R. Bula,⁷¹ J. A. Ernst,⁷¹ V. Jain,⁷¹ B. Pan,⁷¹ M. A. Saeed,⁷¹ F. R. Wappler,⁷¹ S. B. Zain,⁷¹ W. Bugg,⁷² M. Krishnamurthy,⁷² S. M. Spanier,⁷² R. Eckmann,⁷³ J. L. Ritchie,⁷³ A. Satpathy,⁷³ C. J. Schilling,⁷³ R. F. Schwitters,⁷³ J. M. Izen,⁷⁴ X. C. Lou,⁷⁴ S. Ye,⁷⁴ F. Bianchi,⁷⁵ F. Gallo,⁷⁵ D. Gamba,⁷⁵ M. Bomben,⁷⁶ L. Bosisio,⁷⁶ C. Cartaro,⁷⁶ F. Cossutti,⁷⁶ G. Della Ricca,⁷⁶ S. Dittongo,⁷⁶ L. Lanceri,⁷⁶ L. Vitale,⁷⁶ V. Azzolini,⁷⁷ F. Martinez-Vidal,⁷⁷ Sw. Banerjee,⁷⁸ B. Bhuyan,⁷⁸ C. M. Brown,⁷⁸ D. Fortin,⁷⁸ K. Hamano,⁷⁸ R. Kowalewski,⁷⁸ I. M. Nugent,⁷⁸ J. M. Roney,⁷⁸ R. J. Sobie,⁷⁸ J. J. Back,⁷⁹ P. F. Harrison,⁷⁹ T. E. Latham,⁷⁹ G. B. Mohanty,⁷⁹ M. Pappagallo,⁷⁹ H. R. Band,⁸⁰ X. Chen,⁸⁰ B. Cheng,⁸⁰ S. Dasu,⁸⁰ M. Datta,⁸⁰ K. T. Flood,⁸⁰ J. J. Hollar,⁸⁰ P. E. Kutter,⁸⁰ B. Mellado,⁸⁰ A. Mihalyi,⁸⁰ Y. Pan,⁸⁰ M. Pierini,⁸⁰ R. Prepost,⁸⁰ S. L. Wu,⁸⁰ Z. Yu,⁸⁰ and H. Neal⁸¹

(BABAR Collaboration)

¹Laboratoire de Physique des Particules, F-74941 Annecy-le-Vieux, France

²Universitat de Barcelona, Facultat de Fisica Dept. ECM, E-08028 Barcelona, Spain

³Università di Bari, Dipartimento di Fisica and INFN, I-70126 Bari, Italy

⁴Institute of High Energy Physics, Beijing 100039, China

⁵University of Bergen, Institute of Physics, N-5007 Bergen, Norway

⁶Lawrence Berkeley National Laboratory and University of California, Berkeley, California 94720, USA

⁷University of Birmingham, Birmingham, B15 2TT, United Kingdom

⁸Ruhr Universität Bochum, Institut für Experimentalphysik I, D-44780 Bochum, Germany

⁹University of Bristol, Bristol BS8 1TL, United Kingdom

¹⁰University of British Columbia, Vancouver, British Columbia, Canada V6T 1Z1

¹¹Brunel University, Uxbridge, Middlesex UB8 3PH, United Kingdom

¹²Budker Institute of Nuclear Physics, Novosibirsk 630090, Russia

¹³University of California at Irvine, Irvine, California 92697, USA

¹⁴University of California at Los Angeles, Los Angeles, California 90024, USA

¹⁵University of California at Riverside, Riverside, California 92521, USA

¹⁶University of California at San Diego, La Jolla, California 92093, USA

¹⁷University of California at Santa Barbara, Santa Barbara, California 93106, USA

¹⁸University of California at Santa Cruz, Institute for Particle Physics, Santa Cruz, California 95064, USA

¹⁹California Institute of Technology, Pasadena, California 91125, USA

²⁰University of Cincinnati, Cincinnati, Ohio 45221, USA

²¹University of Colorado, Boulder, Colorado 80309, USA

²²Colorado State University, Fort Collins, Colorado 80523, USA

²³Universität Dortmund, Institut für Physik, D-44221 Dortmund, Germany

²⁴Technische Universität Dresden, Institut für Kern- und Teilchenphysik, D-01062 Dresden, Germany

- ²⁵*Ecole Polytechnique, Laboratoire Leprince-Ringuet, F-91128 Palaiseau, France*
- ²⁶*University of Edinburgh, Edinburgh EH9 3JZ, United Kingdom*
- ²⁷*Università di Ferrara, Dipartimento di Fisica and INFN, I-44100 Ferrara, Italy*
- ²⁸*Laboratori Nazionali di Frascati dell'INFN, I-00044 Frascati, Italy*
- ²⁹*Università di Genova, Dipartimento di Fisica and INFN, I-16146 Genova, Italy*
- ³⁰*Harvard University, Cambridge, Massachusetts 02138, USA*
- ³¹*Universität Heidelberg, Physikalisches Institut, Philosophenweg 12, D-69120 Heidelberg, Germany*
- ³²*Imperial College London, London, SW7 2AZ, United Kingdom*
- ³³*University of Iowa, Iowa City, Iowa 52242, USA*
- ³⁴*Iowa State University, Ames, Iowa 50011-3160, USA*
- ³⁵*Johns Hopkins University, Baltimore, Maryland 21218, USA*
- ³⁶*Universität Karlsruhe, Institut für Experimentelle Kernphysik, D-76021 Karlsruhe, Germany*
- ³⁷*Laboratoire de l'Accélérateur Linéaire, IN2P3-CNRS et Université Paris-Sud 11, Centre Scientifique d'Orsay, B.P. 34, F-91898 ORSAY Cedex, France*
- ³⁸*Lawrence Livermore National Laboratory, Livermore, California 94550, USA*
- ³⁹*University of Liverpool, Liverpool L69 7ZE, United Kingdom*
- ⁴⁰*Queen Mary, University of London, E1 4NS, United Kingdom*
- ⁴¹*University of London, Royal Holloway and Bedford New College, Egham, Surrey TW20 0EX, United Kingdom*
- ⁴²*University of Louisville, Louisville, Kentucky 40292, USA*
- ⁴³*University of Manchester, Manchester M13 9PL, United Kingdom*
- ⁴⁴*University of Maryland, College Park, Maryland 20742, USA*
- ⁴⁵*University of Massachusetts, Amherst, Massachusetts 01003, USA*
- ⁴⁶*Massachusetts Institute of Technology, Laboratory for Nuclear Science, Cambridge, Massachusetts 02139, USA*
- ⁴⁷*McGill University, Montréal, Québec, Canada H3A 2T8*
- ⁴⁸*Università di Milano, Dipartimento di Fisica and INFN, I-20133 Milano, Italy*
- ⁴⁹*University of Mississippi, University, Mississippi 38677, USA*
- ⁵⁰*Université de Montréal, Physique des Particules, Montréal, Québec, Canada H3C 3J7*
- ⁵¹*Mount Holyoke College, South Hadley, Massachusetts 01075, USA*
- ⁵²*Università di Napoli Federico II, Dipartimento di Scienze Fisiche and INFN, I-80126, Napoli, Italy*
- ⁵³*NIKHEF, National Institute for Nuclear Physics and High Energy Physics, NL-1009 DB Amsterdam, The Netherlands*
- ⁵⁴*University of Notre Dame, Notre Dame, Indiana 46556, USA*
- ⁵⁵*Ohio State University, Columbus, Ohio 43210, USA*
- ⁵⁶*University of Oregon, Eugene, Oregon 97403, USA*
- ⁵⁷*Università di Padova, Dipartimento di Fisica and INFN, I-35131 Padova, Italy*
- ⁵⁸*Universités Paris VI et VII, Laboratoire de Physique Nucléaire et de Hautes Energies, F-75252 Paris, France*
- ⁵⁹*University of Pennsylvania, Philadelphia, Pennsylvania 19104, USA*
- ⁶⁰*Università di Perugia, Dipartimento di Fisica and INFN, I-06100 Perugia, Italy*
- ⁶¹*Università di Pisa, Dipartimento di Fisica, Scuola Normale Superiore and INFN, I-56127 Pisa, Italy*
- ⁶²*Prairie View A&M University, Prairie View, Texas 77446, USA*
- ⁶³*Princeton University, Princeton, New Jersey 08544, USA*
- ⁶⁴*Università di Roma La Sapienza, Dipartimento di Fisica and INFN, I-00185 Roma, Italy*
- ⁶⁵*Universität Rostock, D-18051 Rostock, Germany*
- ⁶⁶*Rutherford Appleton Laboratory, Chilton, Didcot, Oxon, OX11 0QX, United Kingdom*
- ⁶⁷*DSM/Dapnia, CEA/Saclay, F-91191 Gif-sur-Yvette, France*
- ⁶⁸*University of South Carolina, Columbia, South Carolina 29208, USA*
- ⁶⁹*Stanford Linear Accelerator Center, Stanford, California 94309, USA*
- ⁷⁰*Stanford University, Stanford, California 94305-4060, USA*
- ⁷¹*State University of New York, Albany, New York 12222, USA*
- ⁷²*University of Tennessee, Knoxville, Tennessee 37996, USA*
- ⁷³*University of Texas at Austin, Austin, Texas 78712, USA*
- ⁷⁴*University of Texas at Dallas, Richardson, Texas 75083, USA*
- ⁷⁵*Università di Torino, Dipartimento di Fisica Sperimentale and INFN, I-10125 Torino, Italy*
- ⁷⁶*Università di Trieste, Dipartimento di Fisica and INFN, I-34127 Trieste, Italy*
- ⁷⁷*IFIC, Universitat de Valencia-CSIC, E-46071 Valencia, Spain*
- ⁷⁸*University of Victoria, Victoria, British Columbia, Canada V8W 3P6*
- ⁷⁹*Department of Physics, University of Warwick, Coventry CV4 7AL, United Kingdom*

* Also at Laboratoire de Physique Corpusculaire, Clermont-Ferrand, France

† Also with Università di Perugia, Dipartimento di Fisica, Perugia, Italy

‡ Also with Università della Basilicata, Potenza, Italy

⁸⁰University of Wisconsin, Madison, Wisconsin 53706, USA⁸¹Yale University, New Haven, Connecticut 06511, USA

(Received 31 July 2006; published 12 September 2006)

Branching fraction and asymmetry measurements of charmless $B^+ \rightarrow K^{*+} h_1^+ h_2^-$ (where $h_{1,2} = K, \pi$) decays are presented, using a data sample of 232×10^6 $Y(4S) \rightarrow B\bar{B}$ decays collected with the *BABAR* detector at the SLAC PEP-II asymmetric-energy B factory. Using a maximum likelihood fit, the following branching fraction results were obtained: $\mathcal{B}(B^+ \rightarrow K^{*+} K^+ K^-) = (36.2 \pm 3.3 \pm 3.6) \times 10^{-6}$ and $\mathcal{B}(B^+ \rightarrow K^{*+} \pi^+ \pi^-) = (75.3 \pm 6.0 \pm 8.1) \times 10^{-6}$. Upper limits were set for $\mathcal{B}(B^+ \rightarrow K^{*+} \pi^+ K^-) < 11.8 \times 10^{-6}$ and $\mathcal{B}(B^+ \rightarrow K^{*+} K^+ \pi^-) < 6.1 \times 10^{-6}$ at 90% confidence level. The charge asymmetries for the decays $B^+ \rightarrow K^{*+} K^+ K^-$ and $B^+ \rightarrow K^{*+} \pi^+ \pi^-$ were measured to be $\mathcal{A}_{K^+ K^+ K^-} = 0.11 \pm 0.08 \pm 0.03$ and $\mathcal{A}_{K^+ \pi^+ \pi^-} = 0.07 \pm 0.07 \pm 0.04$, respectively. The first error quoted on branching fraction and asymmetry measurements is statistical and the second systematic.

DOI: 10.1103/PhysRevD.74.051104

PACS numbers: 13.25.Hw, 11.30.Er, 12.15.Hh

Charmless decays of B mesons to three-body final states are very important in aiding the understanding of the weak interaction and complex quark couplings described by the Cabibbo-Kobayashi-Maskawa (CKM) matrix elements [1]. Improved experimental measurements of these charmless decays, combined with theoretical developments, can provide significant constraints on the CKM matrix parameters or uncover evidence for physics beyond the standard model. For example, the branching fraction of the decay $B^+ \rightarrow K^{*+} \pi^+ K^-$ is sensitive to CKM matrix elements V_{td} and V_{ub} (see Fig. 1). Additionally, a $B^+ \rightarrow K^{*+} \pi^+ K^-$ branching fraction value equal to or smaller than the branching fraction of the standard model suppressed decay $B^+ \rightarrow K^{*+} K^+ \pi^-$ would be an indication of new physics.

We identify K^{*+} mesons through their decay to $K_S^0 \pi^+$. Charged B -meson decays to $K_S^0 \pi^+ h_1^+ h_2^-$ (where $h_{1,2} = K$ or π) are dominated by $K^{*+} h_1^+ h_2^-$, but can also proceed via a nonresonant component as well as through observed intermediate charmless resonances such as $B^+ \rightarrow K^{*+} \phi$ or $B^+ \rightarrow K^{*+} \rho^0$ [2–4], or other as-yet-unobserved intermediate charmless resonances. To date, there are only limits on the charmless decays $B^+ \rightarrow K^{*+} h_1^+ h_2^-$, measured by the ARGUS experiment [5] using less than 0.2 fb^{-1} .

Asymmetry measurements of charmless B decays can be used to probe for CP violation where the CP asymmetry is defined as:

$$\mathcal{A}_{K^* h_1 h_2} = \frac{\Gamma_{K^{*+} h_1^- h_2^+} - \Gamma_{K^{*+} h_1^+ h_2^-}}{\Gamma_{K^{*+} h_1^- h_2^+} + \Gamma_{K^{*+} h_1^+ h_2^-}}, \quad (1)$$

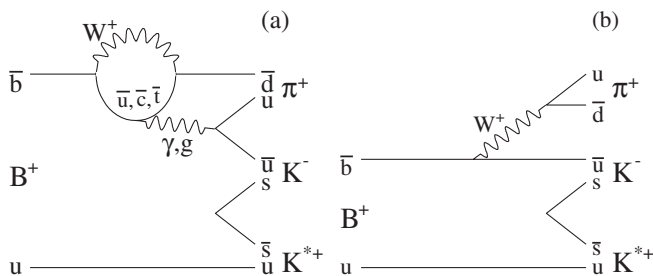


FIG. 1. Penguin (a) and tree (b) Feynman diagrams for the decay $B^+ \rightarrow K^{*+} \pi^+ K^-$.

and Γ is the partial width of the charged B decay in the subript.

In the analyses presented in this paper, branching fractions of $B^+ \rightarrow K^{*+} K^+ K^-$ and $B^+ \rightarrow K^{*+} \pi^+ \pi^-$ were measured for the first time, and upper limits were set for $B^+ \rightarrow K^{*+} \pi^+ K^-$ and the standard model suppressed decay $B^+ \rightarrow K^{*+} K^+ \pi^-$, where charge-conjugate decays are also implied. The selection criteria required events with a reconstructed $K_S^0 \pi^+ h_1^+ h_2^-$ final state such that the total charmless contribution to the $K^{*+} h_1^+ h_2^-$ Dalitz plot could be measured (with charmed and charmonium resonances removed), including contributions from resonant charmless substructure. Finally, the $\mathcal{A}_{K^* h_1 h_2}$ values for the observed decays $B^+ \rightarrow K^{*+} K^+ K^-$ and $B^+ \rightarrow K^{*+} \pi^+ \pi^-$ were measured.

The data used in this analysis were collected at the PEP-II asymmetric-energy $e^+ e^-$ storage ring with the *BABAR* detector [6]. The *BABAR* detector consists of a double-sided five-layer silicon tracker, a 40-layer drift chamber, a Cherenkov detector, an electromagnetic calorimeter and a magnet with instrumented flux return. The data sample has an integrated luminosity of 210 fb^{-1} collected at the $Y(4S)$ resonance, which corresponds to $(231.8 \pm 2.5) \times 10^6$ $B\bar{B}$ pairs. It was assumed that the $Y(4S)$ decayed equally to neutral and charged B -meson pairs. In addition, 21.6 fb^{-1} of data collected at 40 MeV below the $Y(4S)$ resonance were used for background studies.

Candidate B mesons were reconstructed from three tracks and a K_S^0 , where the K_S^0 was reconstructed from $\pi^+ \pi^-$ candidates. Each of the three tracks that were not associated with the K_S^0 were required to have at least 12 hits in the drift chamber, a transverse momentum greater than $100 \text{ MeV}/c$ and to be consistent with originating from the beam-spot. These tracks were identified as either pion or kaon candidates using energy loss (dE/dx) measured in the tracking system and the number of photons measured by the Cherenkov detector and their corresponding Cherenkov angles. Furthermore, the tracks were required to fail the electron selection based on dE/dx information, their ratio of energy in the calorimeter to momentum in the drift chamber, and the shower shape of the signal in the calo-

rimeter. The K_S^0 candidates were required to have a reconstructed mass within $15 \text{ MeV}/c^2$ of the nominal K^0 mass [7], a decay vertex separated from the B^+ decay vertex by at least 5 standard deviations, and a cosine of the angle between the line joining the B and K_S^0 decay vertices and the K_S^0 momentum greater than 0.999.

To characterize signal events, three kinematic variables and one event-shape variable were used. The first kinematic variable ΔE , is the difference between the center-of-mass (CM) energy of the B -candidate and $\sqrt{s}/2$, where \sqrt{s} is the total CM energy. The second is the beam-energy-substituted mass $m_{\text{ES}} = \sqrt{(s/2 + \mathbf{p}_i \cdot \mathbf{p}_B)^2/E_i^2 - \mathbf{p}_B^2}$, where \mathbf{p}_B is the B momentum and (E_i, \mathbf{p}_i) is the four-momentum of the $\Upsilon(4S)$ in the laboratory frame. The third kinematic variable is the $K_S^0 \pi^+$ invariant mass, m_{K^*} , used to identify K^{*+} candidates. Using these three kinematic variables, candidates were required to be in the ranges $|\Delta E| < 0.1 \text{ GeV}$, $5.25 < m_{\text{ES}} < 5.29 \text{ GeV}/c^2$ and $0.772 < m_{K^*} < 0.992 \text{ GeV}/c^2$. The event-shape variable is a Fisher discriminant (\mathcal{F}) [8], constructed from a linear combination of the cosine of the angle between the B -candidate momentum and the beam axis, the cosine of the angle between the B -candidate daughters thrust axis and the beam axis, and the zeroth and second angular moments of energy flow about the thrust axis of the reconstructed B .

Continuum quark production ($e^+e^- \rightarrow q\bar{q}$ where $q = u, d, s, c$) was the dominant source of background. This was suppressed using another event-shape variable which was the cosine of the angle θ_T between the thrust axis of the selected B -candidate and the thrust axis of the rest of the event. For continuum background, the distribution $|\cos\theta_T|$ is strongly peaked towards unity whereas the distribution is flat for signal events. Therefore, the relative amount of continuum background was reduced by requiring $|\cos\theta_T| < 0.8$.

Simulated Monte Carlo (MC) events were used to study background from other B -meson decays. The largest B -background for $B^+ \rightarrow K^{*+} \pi^+ \pi^-$ candidates comes from decays including charmonium mesons such as $J/\psi K^{*+}$, $\chi_{c0} K^{*+}$ and $\psi(2S) K^{*+}$, where the charmonium meson decays to $\mu^+ \mu^-$ which are misidentified as pions, or where the charmonium meson decays directly to $\pi^+ \pi^-$. These background events were removed by vetoing reconstructed $\pi^+ \pi^-$ masses in the range $3.04 < m_{\pi^+ \pi^-} < 3.17 \text{ GeV}/c^2$, $3.32 < m_{\pi^+ \pi^-} < 3.53 \text{ GeV}/c^2$ and $3.60 < m_{\pi^+ \pi^-} < 3.78 \text{ GeV}/c^2$, identifying the J/ψ , χ_{c0} and $\psi(2S)$ mesons, respectively. For $B^+ \rightarrow K^{*+} K^+ K^-$ candidates, $J/\psi K^+$ and $\chi_{c0} K^{*+}$ events were removed by rejecting events with a reconstructed invariant mass in the range $3.04 < m_{K^+ K^-} < 3.17 \text{ GeV}/c^2$ and $3.32 < m_{K^+ K^-} < 3.53 \text{ GeV}/c^2$, respectively.

Potential charm contributions from $B^+ \rightarrow \bar{D}^0(\rightarrow K^{*+} h_1^-) h_2^+$ events were removed from corresponding $B^+ \rightarrow K^{*+} h_2^+ h_1^-$ candidates by vetoing events with a re-

constructed $K^{*+} h_1^-$ invariant mass in the range $1.83 < m_{K^* h} < 1.91 \text{ GeV}/c^2$. Additional decays such as $B^+ \rightarrow D^-(\rightarrow K_S^0 \pi^-) \pi^+ \pi^+$ and $B^+ \rightarrow K^{*+} \bar{D}^0(\rightarrow K^+ \pi^-)$ were removed from $B^+ \rightarrow K^{*+} \pi^+ \pi^-$ and $B^+ \rightarrow K^{*+} \pi^+ K^-/K^{*+} K^+ \pi^-$ candidates, respectively, by vetoing events with reconstructed $K\pi$ invariant masses in the range $1.83 < m_{K\pi} < 1.91 \text{ GeV}/c^2$, using the same veto range for \bar{D}^0 and D^+ candidates. Studies of MC events showed that the largest remaining charmed background was $B^+ \rightarrow \bar{D}^0(\rightarrow K^{*+} \pi^-) \pi^+$, with 18% of these events passing the veto. Surviving charmed events had a reconstructed D mass outside the veto as a result of using the wrong π^+ , K^+ or K_S^0 which was incorrectly selected from the other B decay in the event.

After the above selection criteria were applied, a fraction of events for all decays had more than one candidate. For those events, one candidate alone was selected by choosing the candidate whose fitted B decay vertex had the smallest χ^2 value. Studies of MC events showed the selection of $B^+ \rightarrow K^{*+} \pi^+ \pi^-$ events produced the largest number of multiple candidates, in 29% of events, where for these multiple candidates the correct one was reconstructed 70% of the time.

After all requirements, there were five main sources of B -background: two-body decays proceeding via a charmonium meson; two and three-body decays proceeding via a D meson; combinatorial background from three unrelated particles ($K^{*+} h_1^+ h_2^-$); charmless two or four-body B decays with an extra or missing particle and three-body decays with one or more particles misidentified. Along with selection efficiencies obtained from MC simulation, existing branching fractions for these modes [9] were used to estimate their background contributions which were included in fits to data.

In order to extract the signal event yield for the channel under study, an unbinned extended maximum likelihood fit was used. The likelihood function for N candidates is:

$$\mathcal{L} = \frac{1}{N!} \exp\left(-\sum_{i=1}^M n_i\right) \prod_{j=1}^N \left(\sum_{i=1}^M n_i P_i(\vec{\alpha}, \vec{x}_j)\right), \quad (2)$$

where i and j are integers, M is the number of hypotheses (signal, continuum background and B -background), n_i is the number of events for each hypothesis determined by maximizing the likelihood function and $P_i(\vec{\alpha}, \vec{x}_j)$ is a probability density function (PDF) with the parameters $\vec{\alpha}$ associated with \vec{x} , where \vec{x} can be any of the four variables m_{ES} , ΔE , \mathcal{F} , and m_{K^*} . The PDF is a product $P_i(\vec{\alpha}, \vec{x}) = P_i(\vec{\alpha}_{m_{\text{ES}}}, m_{\text{ES}}) \cdot P_i(\vec{\alpha}_{\Delta E}, \Delta E) \cdot P_i(\vec{\alpha}_{\mathcal{F}}, \mathcal{F}) \cdot P_i(\vec{\alpha}_{m_{K^*}}, m_{K^*})$. Studies of MC simulations showed correlations between these variables were small for signal and continuum background hypotheses. However for B -background, correlations were observed between m_{ES} and ΔE , which were taken into account by forming a 2-dimensional PDF for these variables. The parameters of the signal and

B -background PDFs were determined from MC simulation. The continuum background parameters were allowed to vary in the fit, to help reduce systematic effects from this dominant event type. Upper sideband data, defined to be in the region $0.1 < \Delta E < 0.3$ GeV and $5.25 < m_{ES} < 5.29$ GeV/ c^2 , was used to model the continuum background PDFs. For the m_{ES} PDFs, a Gaussian distribution was used for signal, a threshold function [10] for continuum and the combination of a Gaussian and threshold function for B -background. For the ΔE PDFs, a sum of two Gaussian distributions with the same mean was used for the signal, a first-order polynomial for the continuum background and the combination of the two Gaussians and a first-order polynomial was used for B -background. The \mathcal{F} signal, continuum and B -background PDFs were described using the sum of two Gaussian distributions with distinct means and widths. Finally for m_{K^*} PDFs, the sum of a Breit-Wigner and a first-order polynomial was used to describe the signal, continuum and B -background distributions. The first-order polynomial component of the m_{K^*} PDFs was used to model misreconstructed events for signal and background.

In order to allow uncertainties and corrections due to MC simulation to be calculated and applied to the signal modes under study, the decay $B^+ \rightarrow \bar{D}^0(\rightarrow K^{*+} \pi^-) \pi^+$ was used as a calibration channel. These events were selected using the $B^+ \rightarrow K^{*+} \pi^+ \pi^-$ selection criteria, but requiring the reconstructed $K^{*+} \pi^-$ invariant mass be in the range $1.84 < m_{K^{*+} \pi^-} < 1.88$ GeV/ c^2 . With more than 1800 signal events and approximately a 4 to 1 signal to background ratio in the total number of $B^+ \rightarrow \bar{D}^0(\rightarrow K^{*+} \pi^-) \pi^+$ candidates, it was possible to fit the signal PDF parameters for this mode.

Branching fractions, \mathcal{B} , are usually calculated using the following equation, $\mathcal{B} = n_{\text{sig}}/(N_{B\bar{B}} \times \epsilon)$, where n_{sig} is the fitted number of signal events, ϵ is the average signal efficiency obtained from MC simulation and $N_{B\bar{B}}$ is the total number of $B\bar{B}$ events. For the charmless $B^+ \rightarrow K^{*+} h_1^+ h_2^-$ branching fraction, the average efficiency cannot be taken directly from MC events. This was because the efficiency varies over the Dalitz plane and the distribution of events in the Dalitz plane is unknown before fits to data. To calculate the branching fraction, a weight was assigned to each event, j , as:

$$\mathcal{W}_j = \frac{\sum_i V_{\text{sig},i} P_i(\vec{\alpha}, \vec{x}_j)}{\sum_k n_k P_k(\vec{\alpha}, \vec{x}_j)}, \quad (3)$$

where k is an integer and $V_{\text{sig},i}$ is the signal row of the covariance matrix obtained from the fit [11]. This procedure is effectively a background subtraction where these weights have the property $\sum_j \mathcal{W}_j = n_{\text{sig}}$. The branching fraction is then calculated as $\mathcal{B} = \sum_j \mathcal{W}_j / (\epsilon_j \times N_{B\bar{B}})$ where ϵ_j (a function of $m_{K^{*+} h_1^-}^2$, $m_{h_1^- h_2^+}^2$ and the $K^{*+} \rightarrow$

$K_S^0 \pi^+$ decay helicity angle, $\mathcal{H}_{K^{*+}}$) varies across phase space and is simulated in bins using over 7×10^6 MC events for each channel. The size of the bins are optimized to provide continuous coverage of the efficiency distribution.

Figure 2 shows the fitted projections for $B^+ \rightarrow K^{*+} K^+ K^-$, $B^+ \rightarrow K^{*+} \pi^+ K^-$, $B^+ \rightarrow K^{*+} K^+ \pi^-$ and $B^+ \rightarrow K^{*+} \pi^+ \pi^-$ candidates, while the fitted signal yield, measured branching fractions, upper limits and asymmetries are shown in Table I. The candidates in Fig. 2 are signal-enhanced, with a requirement on the probability ratio $\mathcal{P}_{\text{sig}}/(\mathcal{P}_{\text{sig}} + \mathcal{P}_{\text{bkg}})$, optimized to enhance the visibility of potential signal, where \mathcal{P}_{sig} and \mathcal{P}_{bkg} are the signal and the total background probabilities, respectively, (computed without using the variable plotted). The 90% confidence level (C.L.) branching fraction upper limits (\mathcal{B}_{UL}) were determined by integrating the likelihood distribution (with systematic uncertainties included) as a function of the branching fraction from 0 to \mathcal{B}_{UL} , so that $\int_0^{\mathcal{B}_{\text{UL}}} \mathcal{L} d\mathcal{B} = 0.9 \int_0^\infty \mathcal{L} d\mathcal{B}$.

Contributions to the branching fraction systematic error are shown in Table II. Errors due to charged tracking efficiency and K_S^0 reconstruction efficiency were assigned by comparing control channels in MC events and data. The

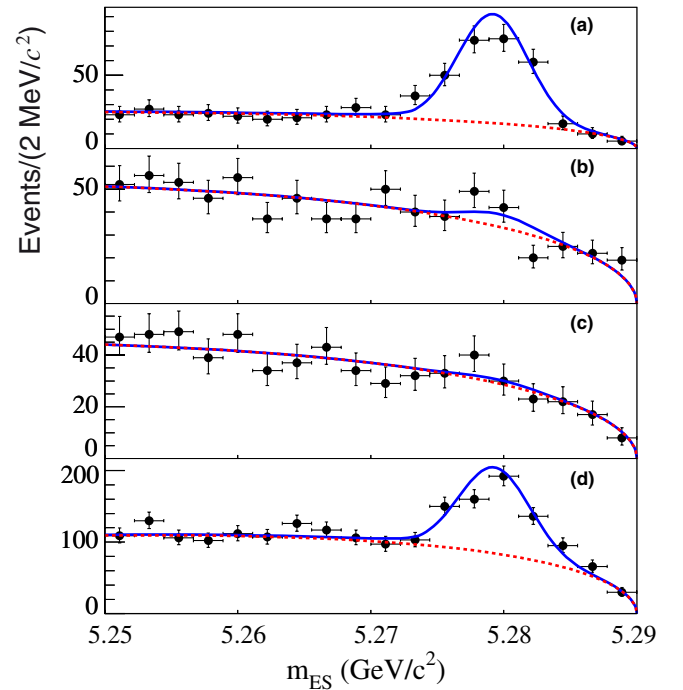


FIG. 2 (color online). Maximum likelihood fit projections of m_{ES} for signal-enhanced samples of charmless $B^+ \rightarrow K^{*+} h_1^+ h_2^-$ candidates. The dashed line is the fitted background PDF while the solid line is the sum of the signal and background PDFs. The points indicate the data. The plot labeled (a) shows a projection of $B^+ \rightarrow K^{*+} K^+ K^-$ candidates, (b) $B^+ \rightarrow K^{*+} \pi^+ K^-$ candidates, (c) $B^+ \rightarrow K^{*+} K^+ \pi^-$ candidates and (d) $B^+ \rightarrow K^{*+} \pi^+ \pi^-$ candidates.

TABLE I. Signal yields, efficiencies and branching fractions for $B^+ \rightarrow K^{*+} K^+ K^-$, $B^+ \rightarrow K^{*+} \pi^+ K^-$, $B^+ \rightarrow K^{*+} K^+ \pi^-$ and $B^+ \rightarrow K^{*+} \pi^+ \pi^-$, measured using $K_S^0 \pi^+ h_1^+ h_2^-$ events. The first error is statistical and in the case of the measured branching fractions the second error is systematic. These efficiencies have taken into account that $\mathcal{B}(K^{*+} \rightarrow K^0 \pi^+) = 2/3$, assuming isospin symmetry, as well as $\mathcal{B}(K^0 \rightarrow K_S^0)$ and $\mathcal{B}(K_S^0 \rightarrow \pi^+ \pi^-)$ [7]. The branching fraction upper limits at a 90% C.L. are shown for $B^+ \rightarrow K^{*+} \pi^+ K^-$ and $B^+ \rightarrow K^{*+} K^+ \pi^-$. Asymmetries are reported (first error is statistical and the second is systematic) only for the channels with statistically significant yields.

Mode	Signal Events Yield	Efficiency (%)	Measured Branching Fraction ($\times 10^{-6}$)	Upper Limit ($\times 10^{-6}$)	Asymmetry (\mathcal{A}_{K^*hh})
$B^+ \rightarrow K^{*+} K^+ K^-$	288 ± 26	3.4	$36.2 \pm 3.3 \pm 3.6$	–	$0.11 \pm 0.08 \pm 0.03$
$B^+ \rightarrow K^{*+} \pi^+ K^-$	20.1 ± 24.7	3.5	$2.5 \pm 3.1 \pm 5.3$	11.8	–
$B^+ \rightarrow K^{*+} K^+ \pi^-$	9.7 ± 17.1	3.5	$1.2 \pm 2.1 \pm 2.0$	6.1	–
$B^+ \rightarrow K^{*+} \pi^+ \pi^-$	583 ± 46	3.3	$75.3 \pm 6.0 \pm 8.1$	–	$0.07 \pm 0.07 \pm 0.04$

error in the efficiency was due to limited MC statistics, generated for each of the decays $B^+ \rightarrow K^{*+} K^+ K^-$, $B^+ \rightarrow K^{*+} \pi^+ K^-$, $B^+ \rightarrow K^{*+} K^+ \pi^-$ and $B^+ \rightarrow K^{*+} \pi^+ \pi^-$. Using a sample of $e^+ e^- \rightarrow \mu^+ \mu^-$ decays, the uncertainty in the number of $B\bar{B}$ events was calculated to be 1.1%. To calculate errors due to the fit procedure, a large number of MC samples were used, containing the amounts of signal and continuum events measured in data, and the estimated number of B -background events. The differences between the generated and fitted values using these samples were used to ascertain the sizes of any biases. Biases of +4.2, +10.7, +5.1 and +6.4% were observed in the fitted signal yields of $B^+ \rightarrow K^{*+} K^+ K^-$, $B^+ \rightarrow K^{*+} \pi^+ K^-$, $B^+ \rightarrow K^{*+} K^+ \pi^-$ and $B^+ \rightarrow K^{*+} \pi^+ \pi^-$, respectively, that were a consequence of small correlations between fit variables. These biases were applied as corrections to obtain the final signal yields and half of the correction was added as a systematic uncertainty. The uncertainty of the B -background contribution to the fit was estimated by

varying the known branching fractions within their errors. Each background was varied individually and the effect on the fitted signal yield was added in quadrature as a contribution to the uncertainty. For the m_{K^*} fit range there was also the possibility of B -background contributions from nonresonant and higher K^{*+} resonances which was modeled in the data fit using a LASS parameterization [12,13]. The contribution from this background was estimated by extrapolating a $K\pi$ invariant mass projection fitted in a higher-mass region ($0.992 < m_{K^*} < 1.6$ GeV/ c^2), into the signal region. This estimated background was modeled in the final data fit, and half of the contribution to the signal was added as a systematic error contribution. The extrapolation assumed there were no integrated interference effects between the $K\pi$ background and the $K^{*+}(892)$ signal. The uncertainty due to reconstructing the wrong $B^+ \rightarrow K^{*+} h_1^+ h_2^-$ signal candidate as a consequence of K/π misidentification, for example $B^+ \rightarrow K^{*+} K^+ K^-$ events being reconstructed as $B^+ \rightarrow K^{*+} \pi^+ K^-$ candidates was deter-

TABLE II. Summary of systematic uncertainty contributions to the branching fraction measurements $B^+ \rightarrow K^{*+} h_1^+ h_2^-$. Multiplicative errors are shown as a percentage of the branching fraction and additive errors are shown in events. The final column shows the total systematic error on the branching fraction.

Error source	$K^{*+} K^+ K^-$ error (%)	$K^{*+} \pi^+ K^-$ error (%)	$K^{*+} K^+ \pi^-$ error (%)	$K^{*+} \pi^+ \pi^-$ error (%)
Multiplicative errors (%)				
Tracking	2.4	2.4	2.4	2.4
K_S^0 Efficiency	1.2	1.2	1.2	1.2
Efficiency	5.3	9.4	8.2	5.6
No. of $B\bar{B}$	1.1	1.1	1.1	1.1
Tot. mult.(%)	6.0	9.8	8.7	6.3
Additive errors (events)				
Fit Bias	6.0	1.1	0.3	18.7
B -background	6.9	33.4	1.3	37.9
$K(892)^{*+}$ bkg	19.5	12.0	4.5	25.6
Signal mis-id	0.0	14.2	15.5	0.0
PDF params.	8.4	19.4	3.0	14.0
Tot. add. (events)	23.1	42.9	16.5	51.4
Total (10^{-6})	3.6	5.3	2.0	8.1

mined using MC events and added as a systematic. The uncertainty due to PDF modeling was estimated from the calibration channel $B^+ \rightarrow \bar{D}^0(\rightarrow K^{*+} \pi^-) \pi^+$ and by varying the PDFs according to the precision of the parameters obtained from the calibration channel fit to data. In order to take correlations between parameters into account, the full correlation matrix was used when varying parameters. All PDF parameters that were originally fixed in the fit were then varied in turn, and each difference from the nominal fit was combined in quadrature and taken as a systematic contribution.

For the decays $B^+ \rightarrow K^{*+} h_1^+ h_2^-$, interference effects between the $K^{*+}(892)$ and S -wave final states (nonresonant and $K_0^{*+}(1430)$) integrate to zero if the acceptance of the detector and analysis is uniform; the same is true of the interference between the $K^{*+}(892)$ and D -wave final states ($K_2^{*+}(1430)$). Studies of MC events showed the efficiency variations were small enough to make these interference effects insignificant. The integrated interference between $K^{*+}(892)$ and other P -wave amplitudes such as $K_1^{*+}(1410)$ is in principle nonzero, but in practice is negligible due to the small branching fraction of $K_1^{*+}(1410) \rightarrow K_S^0 \pi^+$ ($6.6 \pm 1.3\%$) [7] and the fact that the $K\pi$ mass lineshapes have little overlap.

The CP -violating charge asymmetries for the decays $B^+ \rightarrow K^{*+} K^+ K^-$ and $B^+ \rightarrow K^{*+} \pi^+ \pi^-$ were measured to be $\mathcal{A}_{K^*KK} = 0.11 \pm 0.08 \pm 0.03$ and $\mathcal{A}_{K^*\pi\pi} = 0.07 \pm 0.07 \pm 0.04$, respectively, where the first errors are statistical and the second errors are systematic. The background asymmetries $\mathcal{A}_{K^*KK}^{Bkg}$ and $\mathcal{A}_{K^*\pi\pi}^{Bkg}$, which were expected to be consistent with zero, were measured to be 0.00 ± 0.02 and 0.01 ± 0.01 , respectively. As a further study, the asymmetry $\mathcal{A}_{D\pi}$ for $B^+ \rightarrow \bar{D}^0(\rightarrow K^{*+} \pi^-) \pi^+$, also expected to be consistent with zero, was measured to be -0.01 ± 0.02 with a corresponding background asymmetry $\mathcal{A}_{D\pi}^{Bkg}$ of -0.01 ± 0.06 (statistical errors only).

The systematic error on $\mathcal{A}_{K^*h_1h_2}$ was calculated by considering contributions due to track finding, fit biases, B -background uncertainties and particle interaction asymmetries. The error due to fit biases was found to be negligible. Uncertainties due to charged tracking efficiency were assigned by comparing control channels in MC simulation and data. The contribution from B -background was calculated by varying the number of expected events within errors and by assuming a CP -violating asymmetry of ± 0.2 , as there are no available measurements for these decays. The CP asymmetry assumed for the individual B -backgrounds was chosen to be greater than any asymmetry observed for charged B decays. The interaction asymmetry of matter and antimatter with the detector was studied using background measurements $\mathcal{A}_{K^*KK}^{Bkg}$ and $\mathcal{A}_{K^*\pi\pi}^{Bkg}$, where no effect was observed and the statistical precision of the measurement was added as a systematic contribution.

In summary, we have analyzed $K_S^0 \pi^+ h_1^+ h_2^-$ final states to obtain the first branching fraction measurements for the decays $B^+ \rightarrow K^{*+} K^+ K^-$ and $B^+ \rightarrow K^{*+} \pi^+ \pi^-$, and no evidence for new physics was found, placing upper limits on the branching fractions $B^+ \rightarrow K^{*+} \pi^+ K^-$ and $B^+ \rightarrow K^{*+} K^+ \pi^-$.

We are grateful for the excellent luminosity and machine conditions provided by our PEP-II colleagues, and for the substantial dedicated effort from the computing organizations that support *BABAR*. The collaborating institutions wish to thank SLAC for its support and kind hospitality. This work is supported by DOE and NSF (USA), NSERC (Canada), IHEP (China), CEA and CNRS-IN2P3 (France), BMBF and DFG (Germany), INFN (Italy), FOM (The Netherlands), NFR (Norway), MIST (Russia), and PPARC (United Kingdom). Individuals have received support from the Marie Curie EIF (European Union) and the A. P. Sloan Foundation.

-
- [1] N. Cabibbo, Phys. Rev. Lett. **10**, 531 (1963); M. Kobayashi and T. Maskawa, Prog. Theor. Phys. **49**, 652 (1973).
 - [2] B. Aubert *et al.* (*BABAR* Collaboration), Phys. Rev. Lett. **91**, 171802 (2003).
 - [3] B. Aubert *et al.* (*BABAR* Collaboration), hep-ex/0607057.
 - [4] K. F. Chen *et al.* (Belle Collaboration), Phys. Rev. Lett. **94**, 221804 (2005).
 - [5] H. Albrecht (ARGUS Collaboration), Phys. Lett. B **262**, 148 (1991).
 - [6] B. Aubert *et al.* (*BABAR* Collaboration), Nucl. Instrum. Methods Phys. Res., Sect. A **479**, 1 (2002).
 - [7] S. Eidelman *et al.* (Particle Data Group), Phys. Lett. B **592**, 1 (2004).
 - [8] R. A. Fisher, Ann. Eugenics **7**, 179 (1936); G. Cowan, *Statistical Data Analysis* (Oxford University Press, New York, 1998), p. 51.
 - [9] Heavy Flavor Averaging Group (HFAG), <http://www.slac.stanford.edu/xorg/hfag/rare/winter06/charmless/index.html>.
 - [10] H. Albrecht *et al.* (ARGUS Collaboration), Z. Phys. C **48**, 543 (1990).
 - [11] M. Pivk and F. R. Le Diberder, Nucl. Instrum. Methods Phys. Res., Sect. A **555**, 356 (2005).
 - [12] D. Aston *et al.*, Nucl. Phys. **B296**, 493 (1988).
 - [13] B. Aubert *et al.* (*BABAR* Collaboration), Phys. Rev. D **72**, 072003 (2005).